Oxyfuel combustion and reactants preheating to enhance turbulent flame stabilization of low calorific blast furnace gas

Abou Bâ, Armelle Cessou, Niomar Marcano, Faustine Panier, Rémi Tsiava, Guillaume Cassarino, Ludovic Ferrand, David Honoré

Oxyfuel combustion and reactants preheating to enhance turbulent flame stabilization of low calorific blast furnace gas

Abou BÂ[1], Armelle CESSOU[1], Niomar MARCANO[2], Faustine PANIER[2], Rémi TSIAVA[2], Guillaume CASSARINO[3], Ludovic FERRAND[3], David HONORE[1*]

[1] Normandie Univ, INSA Rouen, UNIROUEN, CNRS, CORIA, 76000 Rouen, France

[2] Air Liquide CRCD Paris-Saclay, 78354 Les Loges en Josas, France

[3] CMI GreenLine Europe, 78280 Guyancourt, France

[*] Corresponding author
Tel.: +33-232959852
Fax: +33-232959780 .
E-mail address: david.honore@coria.fr

Abstract

The need for the reduction of the environmental impact of combustion systems in terms of pollutant emissions and preservation of non-renewable resources forces to consider the improvement of energy efficiency and to turn towards alternative fuels in industrial combustion furnaces. However, their use may be an issue because of their low calorific value (LCV) compared to traditional natural gas (NG). The present work considers the combination of oxyfuel combustion with fuel and/or oxygen preheating in order to increase thermal efficiency by heat recovery and enhance LCV oxyfuel flame stabilization, without using a supporting fuel as NG. The study is focused on Blast Furnace Gas (BFG) which has one-tenth the heating value of NG.

This assessment starts with thermochemical calculations of major flame properties at several reactant temperatures. Two fundamental flame configurations are simulated: a fully premixed 1D flame for the determination of adiabatic temperature, thermal thickness and laminar burning velocity, and a counter-flow diffusion flame for the determination of extinction strain rates. The results show that significant enhancement of oxyfuel flame properties can be obtained thanks to the preheating of BFG and oxygen. The effect of such preheating is then experimentally studied at laboratory-scale (25 kW) using a tri-coaxial burner generating a non-premixed turbulent BFG-O_2 flame. The burner geometry consists of an annular BFG injection surrounded by an inner central oxygen injection and an external annular oxygen injection. Based on a critical Damköhler number, a theoretical analysis of the stabilization limit for a turbulent diffusion BFG-O_2 flame with preheated reactant is described and used as a criterion to calculate the burner dimensions. Detailed flame characteristics are investigated from measurements of flue gas emissions and OH* chemiluminescence imaging. From these, the analysis of flame stability diagrams as function of reactant velocities, thermal power, oxygen distribution and preheating temperatures points out the limits of flame stability and the stable combustion regimes achieved at the different operational conditions. Regarding the emissions, very low levels of pollutant emissions such as CO and NOx are achieved in most cases. Further analysis of the results shows that transitions between the various types of flames are controlled by a critical convection velocity in the BFG - oxygen mixing layer. This is quantified from the measurements and matches with the theoretical prediction. Complementary large-scale experiments are performed on a semi-industrial facility, with identical burner geometry, scaled-up to 180 kW using the velocity criterion. The flames show similar structures as obtained at laboratory scale, demonstrating the benefit of preheated oxyfuel combustion for the stabilization of LCV flames. These results validate the analysis of the physical phenomena controlling the limit of stability of BFG oxyfuel flames, as well as the burner design strategy of preheated oxyfuel combustion adapted to low calorific fuels, and the scale-up criteria used for this particular case.

***Keywords**: oxyfuel combustion ; low calorific fuel ; blast furnace gas ; heat recovery ; preheated combustion ; oxygen*

1. Introduction

The need for the reduction of the environmental impact of combustion systems in terms of pollutant emissions and preservation of primary resources forces to consider the energy efficiency improvement and to turn towards alternative fuels in industrial combustion furnaces. Defined as possible substitutes to fossil fuels, gaseous alternative fuels comprise several kinds of fuels, such as: syngas issued from biomass, landfill biogas, by-products gas from industrial plants, etc. Despite the large variation of their compositions, one common feature of these alternative fuels is their low calorific value that has a strong impact on flame stabilization and pollutant emissions. The present study is focused on blast furnace gas (BFG) produced in the steel making industry, which has one of the lowest calorific value within the alternative fuel gases, due to the large concentration of inert gases on its composition. The BFG is known to be one of the most difficult by-product fuels to provide stable flame and safe combustion [Komori 2003, Li 2015, Giles 2016]. In practical applications, BFG is usually burn with supported fuel such as natural gas [Gicquel 2003], or coke oven gas [Hou 2011]. Even if using pure oxygen as oxidizer enhances flame stabilization due to the absence of inert nitrogen, oxyfuel combustion of BFG may still require the support of high calorific fuel [Paubel 2007]. From an energetic point of view, air preheating by flue gases heat recovery is a convenient way to increase global thermal efficiency of combustion units, and also to enhance flame stabilization. Such heat recuperative systems have been recently developed to preheat pure oxygen for applications in glass meting furnaces [Joumani 2010]. Moreover, preheating of BFG can be also envisaged to enhance flame stabilization [Moon 2014].

In this context, the present work studies the effect of the combination of oxyfuel combustion and reactants preheating for turbulent flame stabilization with low calorific value. The initial step includes thermochemical calculations of oxyfuel BFG flames performed at several reactant initial temperatures to quantify the potential benefit of these parameters. A theoretical analysis of the stability for a BFG-O_2 diffusion flame in the shear layer is used to design a tri-coaxial burner. Following to this, the physical phenomena leading the BFG-O_2 turbulent flame stability are experimentally studied using OH* chemiluminescence imaging and flue gas emissions measurements. Lastly, up-scaling effect is characterized from complementary experiments performed on a semi-industrial facility.

2. Oxyflames properties of several low calorific value (LCV) fuels

Table 1 compares BFG compositions and characteristics to three other alternative fuels: biogas, syngas, coke oven gas (COG) and methane. BFG is characterized by its high concentration of inert species (N_2, CO_2), the absence of methane and a very low H_2 content. It has also very low calorific value corresponding to one-tenth the one of methane. These characteristics lead to very low laminar burning velocities S_L (Figure 1), as obtained from simulation of a mono-dimensional stationary and stabilized laminar premixed flame at 298 K and atmospheric pressure, using the COSILAB® software. As no detailed kinetic mechanism has been yet validated in such specific conditions of oxyfuel combustion of LCV gases with fuel and oxygen preheating, initially, this simulation was performed using four different mechanisms such as GRI Mech 3.0, Davis, OpenSmoke and Sun mechanisms, with no major differences between the results [Bâ 2015, Bâ 2017]. The Davis mechanism [Davis 2005], however, initially developed and validated for CO and H_2 fuel mixtures, has been chosen since it has been validated at the closest conditions of fuels composition and reactant temperature [Wang 2012].

Table 1. Compositions and main properties of typical biogas, syngas, coke even gas (COG) and blast furnace gas (BFG) compared to methane

Fuel		Methane	Biogas	Syngas	COG	BFG
Concentrations (% vol.)	**CH_4**	100	52	7	28	-
	H_2	-	-	9	62	5
	CO	-	-	14	6	23
	CO_2	-	40	20	4	23
	N_2	-	8	50	-	49
Net Calorific Value [kWh/m^3(n)]		9.94	5.17	1.44	4.75	0.95
Density [kg/m^3]		0.67	1.20	1.18	0.38	1.27
Stoichiometric mixture fraction Zs [-]		0.34	0.48	0.20	0.24	0.88

The laminar burning velocity S_L with the equivalence ratio is presented on Figure 1 for oxyfuel flames of different fuels such as methane, biogas, syngas, BFG and COG, using the compositions given in Table 1. These are compared to a CH_4-air flame, representative of gaseous fossil fuel (natural gas) combustion with air at ambient temperature as traditional oxidiser. For all these cases, the S_L curve presents the traditional bell shape, but with a maximum on the lean side for the oxyfuel flames, except for COG-O_2 flame. For the latter, very high values of laminar burning velocity are reached because of the large concentration of hydrogen in coke oven gas. Such laminar burning velocity of several meters per second - as for CH_4-O_2 flame - ensures the strength of these oxyfuel flames thanks to the use of pure oxygen as oxidiser. As biogas is a 50:50 mixture of methane with CO_2 and N_2 inert gases (Table 1), the laminar burning velocity of biogas oxyfuel flame is still very high. For syngas-O_2 flame,

the range of S_L is also sufficiently large to ensure flame stabilization when pure oxygen is used as oxidizer. Oxyfuel flames of syngas can then be envisaged with or without reactants preheating for industrial applications, despite its low calorific value. Moreover, operation in the lean conditions can be attractive to reduce NOx emissions, since the burning velocity is still large enough for very lean mixtures. Laminar burning velocity is no longer high for the BFG-O_2 mixture. In this case, S_L is almost constant over the equivalence ratio range calculated [0.4 – 1.3], showing like for the syngas a possible application to lean combustion. However, the S_L values are too moderate to guarantee a reliable use in industrial applications, either without reactant heating or having a support with higher calorific value gases.

These results show that oxyfuel combustion is a convenient technology to guarantee the stabilization of LCV fuels flames as biogas or syngas. However, additional heat supply might be required for BFG flames.

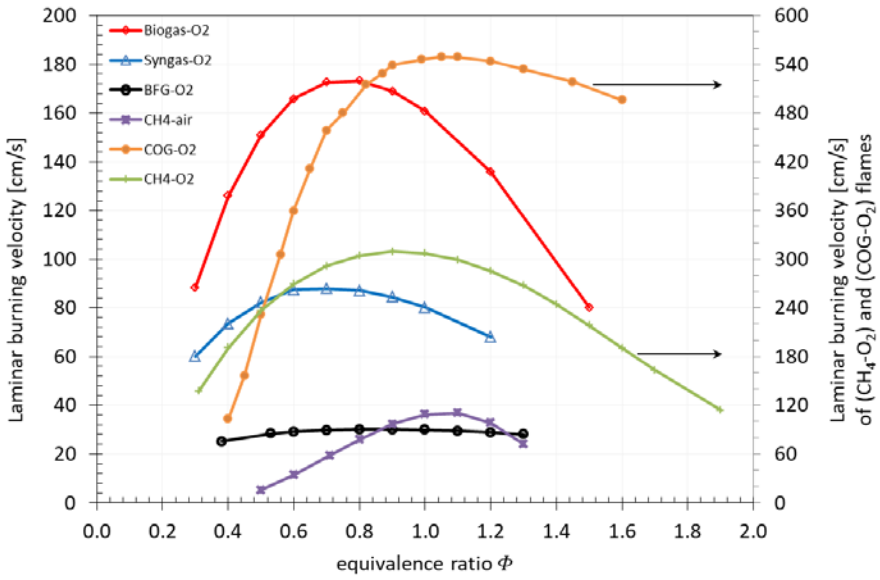

Figure 1. Laminar burning velocity S_L vs. equivalence ratio at ambient temperature (T_{pr} = 300 K) for different oxyfuel flames and a CH_4-air flame. (left axis for biogas-O_2, syngas-O_2,BFG-O_2, and CH_4-air flames – right axis for CH_4-O_2, and COG-O_2 flames).

3. Effects of reactants preheating on BFG oxyfuel flame properties

3.1. Adiabatic temperature and emissions

Figure 2 presents the calculated adiabatic temperature T_{ad} of BFG-O_2 stoichiometric mixture, as well as the major species molar fractions at equilibrium for several preheating temperatures T_{pr}. The adiabatic flame temperature increases quasi-linearly with the temperature, from T_{ad} = 2020 K at T_{pr} = 300 K to T_{ad} = 2325 K at T_{pr} = 900 K. The increase of initial temperature T_{pr} leads to slightly decreases of CO_2 and H_2O molar fractions because of their thermal dissociations, with the correlated increases of CO and H_2 molar fractions in the equilibrium gas composition. The high concentration of nitrogen ([N_2] = 49% vol.) in BFG has a significant impact on NO

formation. This shows that reactants preheating might have a potential impact on pollutant emissions such as CO and NO, and that would have to be considered during development of practical applications.

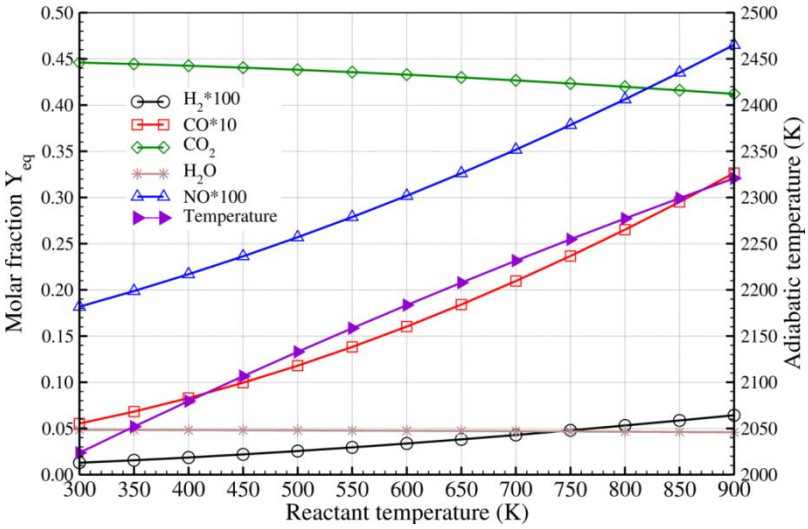

Figure 2. Adiabatic temperature and equilibrium species molar fractions with initial reactant temperature T_{pr} for a BFG-O_2 stoichiometric mixture.

3.2. Laminar burning velocity and flame thickness

Simulations of mono-dimensional freely propagating premixed laminar flames of BFG-O_2 stoichiometric mixtures are performed to determine laminar burning velocity S_L and flame thickness δ_{th}. These properties are essential to evaluate the flame stabilization in the wake of burner nozzle. The laminar burning velocity is useful to compare the reactant conditions in terms of propagating efficiency when a leading-edge occurs. Linked to the heat diffusion, the flame thickness indicates the ability of the flame to be stable in the wake of a lip [Juniper 2003]. Flame thickness is deduced from the temperature profile across the flame front as the ratio between the temperature difference ($T_{ad} - T_{pr}$) and the maximum temperature gradient across the flame front. Figure 3 presents the changes of S_L and δ_{th} as a function of the initial reactant temperature.

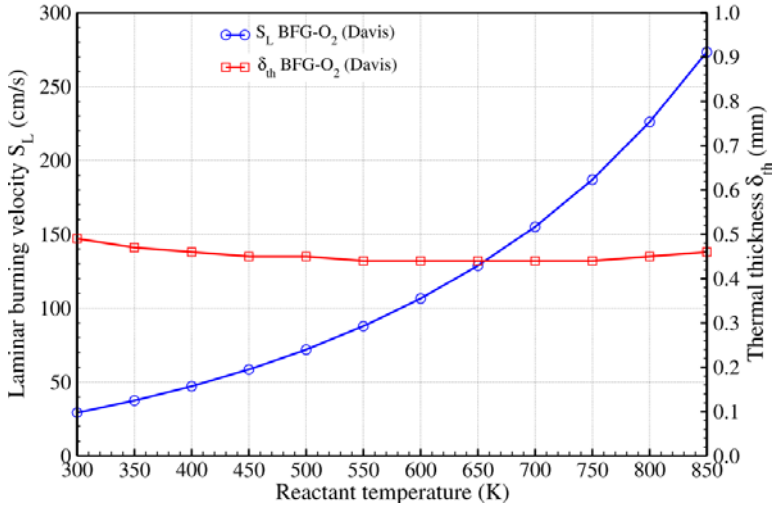

Figure 3. Laminar burning velocity S_L and flame thickness δ_{th} with reactants preheating temperature T_{pr}

The laminar burning velocity becomes nine times higher when T_{pr} varies from 300 K to 850 K. The sensitivity of the S_L with temperature is commonly described by a power law expression such as:

$$\frac{S_L(T_{pr})}{S_L(T_0=300K)} = \left[\frac{T_{pr}}{T_0}\right]^{\alpha} \quad (1)$$

The exponent α in the present case is 1.72. This represents a significant increment in the flame velocity under these conditions, compared to several studies carried out with preheated methane-air flames where the obtained α value was in the range of 1.575 to 1.68. [Mishra 2003, Sharma 1981, Han 2007, Liao 2004, Lamige 2015].

High values of S_L reached with reactants preheating provide a potential to ensure the oxyfuel flame stabilization, even with very low calorific value fuel gas. S_L increases almost one order of magnitude, when the adiabatic temperature change is moderate. Thus, a significant flame stabilization enhancement can be achieved without having a strong impact on the thermal process in an industrial facility.

Without preheating, the flame thickness of BFG-O_2 oxyfuel flame is high, $\delta_{th} \approx 0.5$ mm. When increasing T_{pr}, a slightly decrease is observed. The narrowing of the temperature difference $(T_{ad} - T_{pr})$ due to preheating reactants is compensated by an equivalent decrease of the temperature gradient. Conservation of wide thermal thickness shows that the width of the low velocity zone in the wake of the lip's nozzle has to be kept large enough, as significant interaction between flame front and small turbulent structures can be expected in a turbulent BFG-O_2 flame with such flame thickness [Juniper 2003].

3.3. *Strain rate and flame blow off*

In order to analyze the flame extinction in a turbulent preheated BFG-O_2 system, 1D diffusion counter-flow flame simulations were also carried out. These simulations allowed to highlight the strain effect on the BFG-O_2 flame stability and, to determine the critical strain rate K* where the flame is blown off. In this configuration, the effect of the reactants preheating is studied by considering the same temperature for oxygen and BFG, i.e. on both sides of the diffusion flame. Figure 4 presents the adiabatic diffusion flame temperature when increasing the strain rate at different reactants inlet temperatures.

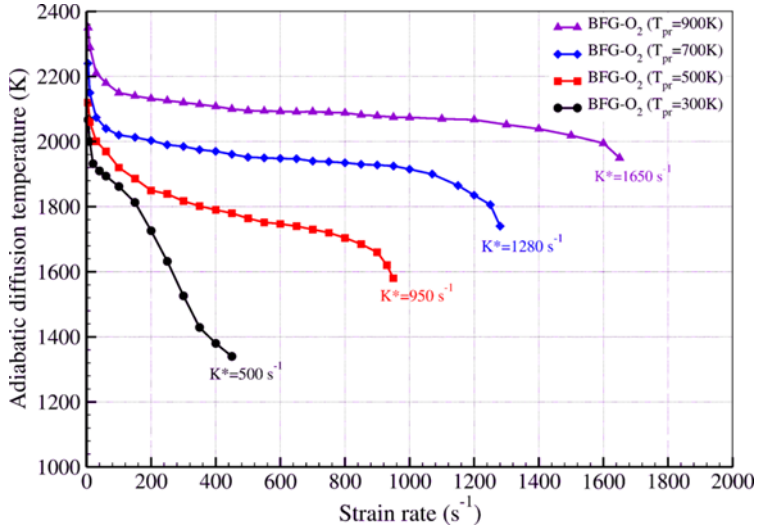

Figure 4. Adiabatic flame temperature T_{ad} ~~vs.~~ with strain rate K ~~of mono-dimensional~~ for 1D counterflow diffusion flames.

For all preheating reactants temperatures, the progressive increase of strain in the diffusion flame induces a decrease of the adiabatic temperature before reaching the flame extinction limit at the corresponding critical strain rate K*.

At ambient temperature, the adiabatic temperature decreases rapidly even from low strain rate values before reaching the limit where the flame is extinguished at K* = 500 s^{-1}, despite the use of oxygen as oxidiser. The reactants preheating leads to larger adiabatic temperature, as already observed in equilibrium calculations, as well as to a significant change in the slope of the adiabatic temperature with the strain rate. After a first decline of adiabatic temperature at low strains, the adiabatic temperature presents a plateau followed up by a second decline, up to the flame extinction limit. The range of strain rate of the plateau is wider at higher reactants temperature, showing in this way an enlarged flame stability limit. The critical strain rate at T_{pr} = 500 K is twice the ambient case (K* = 500 s^{-1}), and more than three times for T_{pr} = 900 K.

All these simulations show the potential benefit of reactants preheating on oxyfuel BFG flame, in terms of flame stabilization and limits to extinguishment. The experimental studies carried out at both laboratory and industrial-scales are devoted to make real demonstrations of this potential.

4. Oxyfuel burner adapted to LCV fuels

4.1. Burner configuration and operating conditions

Based on previous experience of BFG oxyfuel combustion [Paubel 2007], a tri-coaxial burner configuration is chosen, with an annular BFG injection surrounded by a central (O_{2i}) oxygen injection and a peripheral (O_{2e}) oxygen injection (Figure 5). Thus, for fixed LCV fuel composition and global equivalence ratio, the oxygen distribution between the central and external flows will be used to control flame stability and length, heat transfer along the combustion chamber and pollutant emissions in the flue gases.

The oxygen distribution is quantified by a non-dimensional parameter Ro, defined from internal $Q_{O_{2i}}$ and external $Q_{O_{2e}}$ oxygen volumetric flowrates:

$$R_O = \frac{Q_{O_{2i}}}{Q_{O_{2i}} + Q_{O_{2e}}} \quad (2)$$

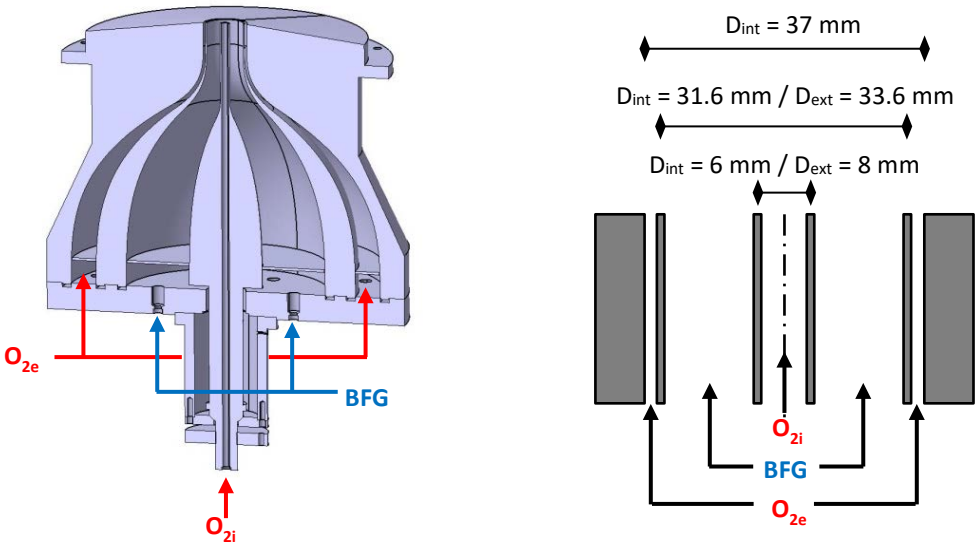

Figure 5. Isometric view of the tri-coaxial O_2 / BFG / O_2 burner (left) and diagram of the burner exit with external and internal diameters of the injections (right)

The burner is manufactured in Inconel 600 stainless steel in order to be able to supply hot gaseous fuels and oxygen. On the bottom of the burner, BFG and oxygen supplies are set longitudinally to avoid any direct impact of hot reactant on burner walls. For each annular flow, the injections impinge on small obstacles to induce their

expansion in the large volumes on the burner base, which then act as plenum chambers to ensure flow homogeneity. Progressive annular flows contractions made by convergent shapes allow to control the velocity profiles at the burner exit.

For lab-scale experiments, the burner is designed for a thermal power of 25 kW and a total equivalence ratio of $\phi = 0.96$. The same burner geometry is also considered for the semi-industrial scale experiments at nominal power of 180 kW. This corresponds to the thermal power target for reheating furnaces in the steel making industry application.

4.2. Original design rules for coaxial LCV burners

Previous experimental study has shown that the stabilization of a BFG-O_2 turbulent diffusion flame at 300 K is controlled by the convection velocity, $U_C = (U_{BFG}+U_{O2})/2$, up to a limit of 10.5 m/s [Paubel 2007]. The stabilisation limit of such BFG-O_2 turbulent diffusion flame at the burner lip can be characterized by a critical Damköhler number Da* which relates the interaction between a representative mixing time scale and the low chemical reactivity of BFG-O_2. Several authors have shown that the stabilisation of a turbulent diffusion flame in the region close to the burner exit is controlled by the burner lip width, which has to be large enough to enable the flame to be tucked in the region of low momentum behind the lip [Takahashi 1990, Juniper 2003, Candel 2006, Okateyama 2009]. Therefore, in the present work, the representative mixing time is defined as; $\tau_t = e/U_c$, associating the width of the burner lip e to the convection velocity U_C related to the large structures developed in the shear layer [Dahm 1992, Takahashi 1990, Rehab 1997, Villermaux 2000]. The chemical time τ_{ch} can be estimated by the scalar dissipation rate χ_q [Peters 2000]:

$$\tau_{ch} = \frac{1}{\chi_q} = \frac{D}{Z_s^2.(1-Z_s)^2.S_L^2} \quad (3)$$

Thus, the expression of the Damköhler number Da is:

$$Da = \frac{\tau_t}{\tau_{ch}} = \frac{e}{U_c} \cdot \frac{Z_s^2.(1-Z_s)^2.S_L^2}{D} \quad (4)$$

In the present work, the value of the critical Damköhler number at 300 K (Da* = 0.004) is adopted as a control parameter of the flame anchorage to the burner lip e and is also used to design the tri-coaxial burner, in order to reach the limit of stability at ambient reactant temperature. First, the chemical time is determined from thermochemical calculations of the diffusivity D, the stoichiometric mixture fraction Z_s and the laminar burning

velocity S_L. The mixing time τ_t depends on the lip width and the convection velocity U_c. Considering that the thermal thickness of BFG-O_2 premixed oxyfuel flame remains constant ($\delta_{th} \approx 0.5$ mm) whatever reactant temperature (Figure 3), the width of the burner lips is chosen equal to 1 mm, in order to favour stabilization of attached BFG-O_2 diffusion flame and to delay the transitions to lifted flame regime and its extinction afterwards [Juniper 2003, Otakeyama 2009].

Following this methodology, the maximum convection velocity U_c^* can be determined for each reactant preheating from the critical Damköhler number (Da* = 0.004). Figure 6 presents the convection velocity according to the reactant preheating temperature T_{pr}. The exponential increase in U_c points out that the reactant preheating will ensure undoubtedly the stabilization of BFG-O_2 turbulent diffusion flames in the inner and outer shear layers. In this tri-coaxial burner geometry, two convection velocities, U_{ci} and U_{ce}, can be defined in the inner (O_{2i}-BFG) and outer (BFG-O_{2e}) mixing layers respectively. Then, dimensions of the injection exit diameters of the lab-scale burner are chosen to have inner U_{ci} and outer U_{ce} convection velocities closed to the critical convection velocity U_c^* at T_{pr} = 300K for nominal operating conditions. Tri-coaxial injections diameters are given in Figure 5. The burner is designed to be at the limit of stability without preheating using the criterion U_c^*, in order to investigate how the reactant preheating enhances the flame stability. Figure 6 illustrates the expected enhancement: when increasing reactant temperature, the linear increases of both U_{ci} and U_{ce} are weak compared to the exponential increase of U_c^*. This should favour the stabilization of BFG-O_2 flames in the inner and outer shear layers.

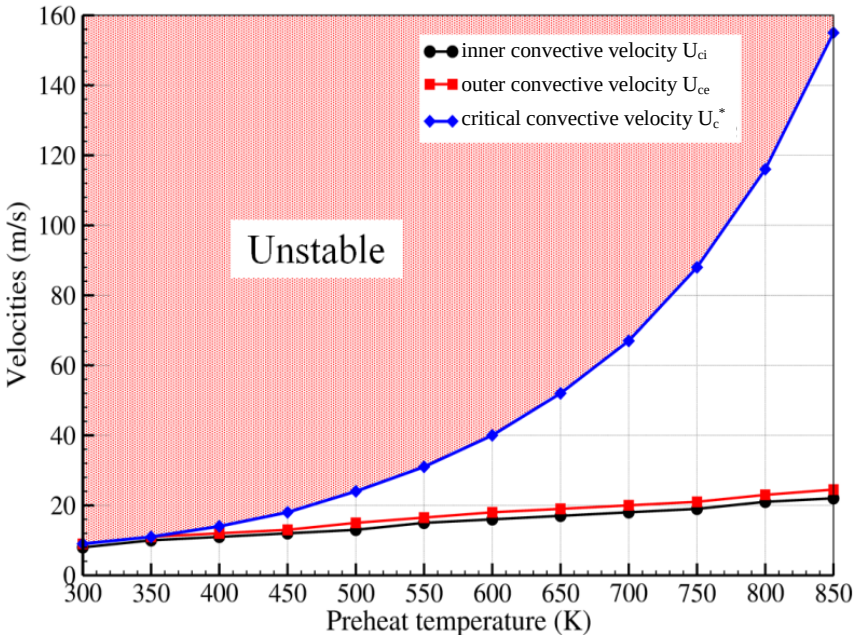

Figure 6. Effect of reactants temperature T_{pr} on BFG-O_{2i} and BFG-O_{2e} convective velocities for the tri-coaxial burner, compared to the critical value of the convection velocity U_c*

5. Experimental study on the lab-scale facility

5.1. Experimental setup

The BFG-O_2 tri-coaxial burner is installed on the lab-scale facility at CORIA laboratory, which consists of a cylindrical combustion chamber (length = 1 m - dia. = 0.4 m) with refractory walls and several optical accesses. The synthetic BFG mixture is provided by a dynamic mixing system of pure gases, controlled by a set of mass flow-meters. Three independent electric heating systems are used to control the preheating of the fuel mixture and the two oxygen supplies for central and outer flows. The facility is instrumented with a gas analyser Siemens Oxymat 61 - Ultramat 23 for on-line measurements of O_2, CO_2, CO_2 and NOx in the flue gases, and several K-type thermocouples are installed close to the combustion chamber wall to obtain longitudinal temperature profile. The structure of BFG-O_2 flame is obtained by OH* chemiluminescence imaging performed through the optical access located close to the burner exit. Chemiluminescence images are collected with a Princeton PI-MAX 4 ICCD camera (1024 x 1024 pixels - 16 bits) equipped with f/2.8 25 mm UV objective lens associated with two Schott UG11 filters. For each flame, a series of 500 instantaneous images, with an exposure time of 100 µs, is recorded in order to determine a representative mean image. The axial symmetry of the burner allows for reconstructing the mean tomographic structure of the BFG-O_2 flame. This is carried out using Abel's inversion post-processing of the average OH* chemiluminescence image.

5.2. Stability diagram and flame structures for ambient reactant temperature

Figure 7 presents the flame stability diagram without any reactants preheating. For a given thermal power, the tests were carried out at a fixed equivalence ratio and increasing the oxygen distribution Ro. The results show that the oxyfuel BFG flame is stabilized in a narrow range of thermal power and oxygen distribution, which are lower than the nominal operating conditions. Slight modifications in the oxygen distribution quickly induce the appearance of fluctuations and disturbances in the flame. Thus, several flame structures are observed from a minimum Ro value of 10%,

For low thermal power, double concentric flames attached to the burner lips are observed. Mean structure of these flames - labelled 'type A' - is presented in Figure 8 by the mean OH* chemiluminescence image integrated along the line of sight, and the corresponding mean tomographic image resulting from the Abel's inversion at the operating conditions corresponding to 12.5kW, Ro of 10% and Tpr of 300K. A diffusion flame is stabilized from the burner exit in both the BFG-O_{2i} and BFG-O_{2e} shear layers. Two types of A flames are distinguished depending

on the CO emissions. For the lowest tested thermal power corresponding to 10 kW, CO concentrations higher than 300 ppm are measured in the flue gas for A1 type flame as in the stability diagram. With slight increments of thermal power to 12.5 kW the CO emission levels are less than 20 ppm, showing that larger flowrates enhance turbulent mixing and ensure complete combustion (A2 flame in the stability diagram). Despite the significant high nitrogen concentration in BFG, NOx emissions are very low (less than 15 ppm) for all flames, thanks to their low heat release density.

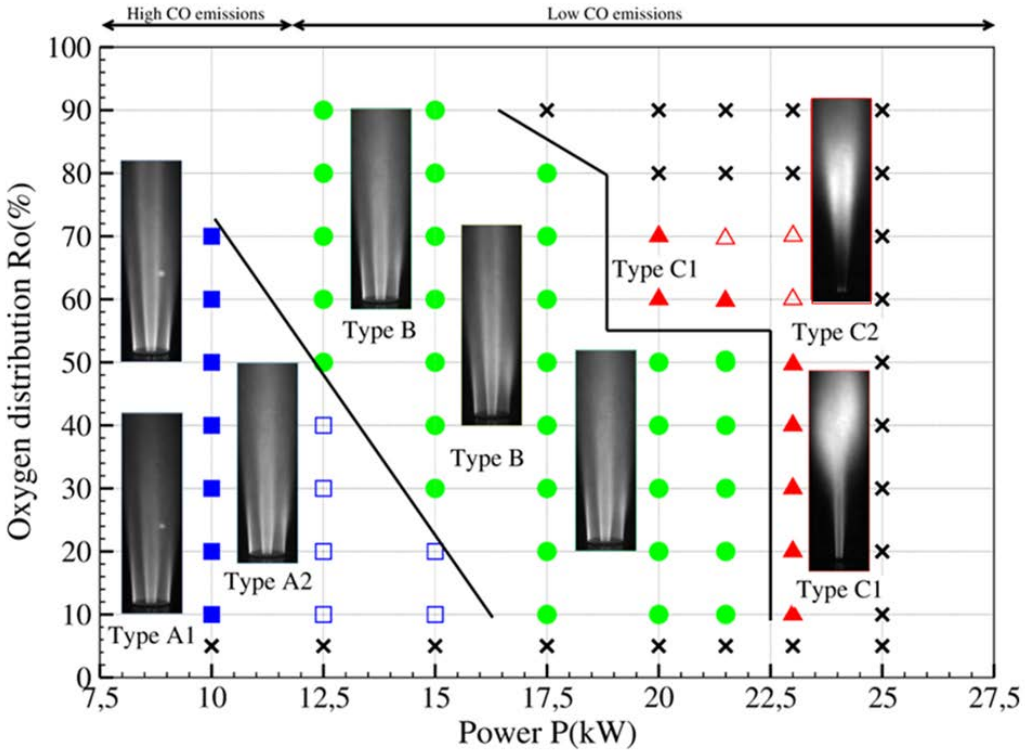

Figure 7. Stability diagram of oxyfuel BFG flames without reactants preheating. (blue filled square: A1 flame - blue open square: A2 flame - green circle: B flame - red filled triangle: C1 flame - red open triangle: C2 flame - black cross: blown-off flame)

When increasing P and/or Ro, double concentric attached flame (A type) still exists up to the first transition, where some local fluctuations of the external annular BFG-O_{2e} flame are observed. For these flames, defined as 'type B' on the stability diagram, the intermittent extinctions generate a dissymmetry in the mean structure of the external annular flame (Figure 9). This effect is even more pronounced when increasing P and/or Ro and lead to a third flame structure, Type C1, where the external flame is lifted-off. For this, the flame stabilization is ensured by the attached central BFG-O_{2i} flame, such as it is shown in Figure 10. For higher thermal power and central oxygen flowrate, some local extinction is observed in the inner BFG-O_{2i} flame, (Type C2 - Figure 11), before it is totally blown-out (see stability diagram in Figure 7).

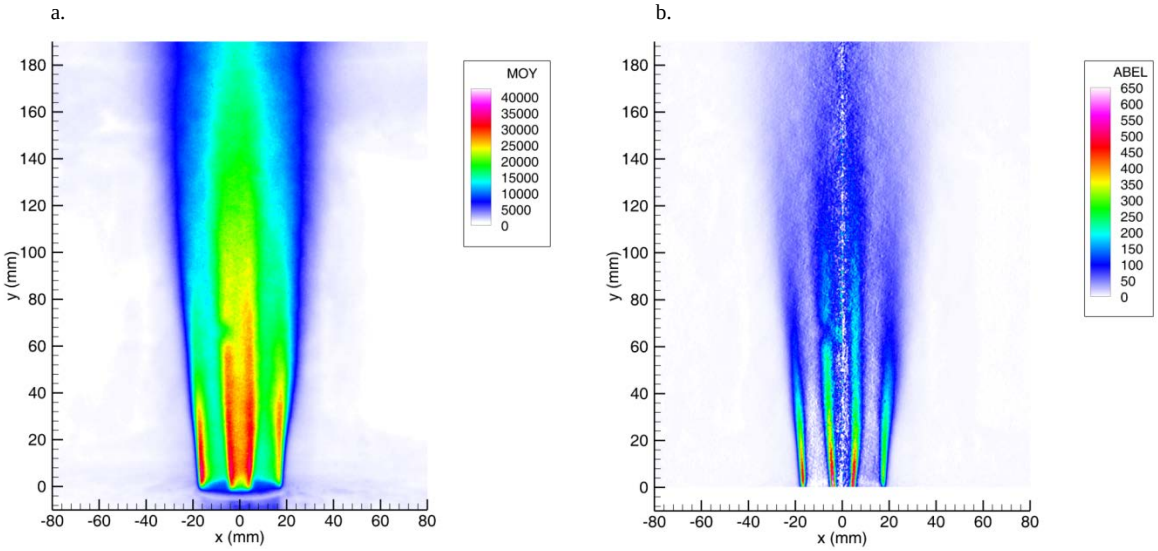

Figure 8. The structure of 'type A' oxyfuel BFG flame for 12.5kW, Ro of 10% and T_{pr} = 300K.
a: Mean OH* chemiluminescence image. b: Tomographic image reconstructed by Abel's inversion.

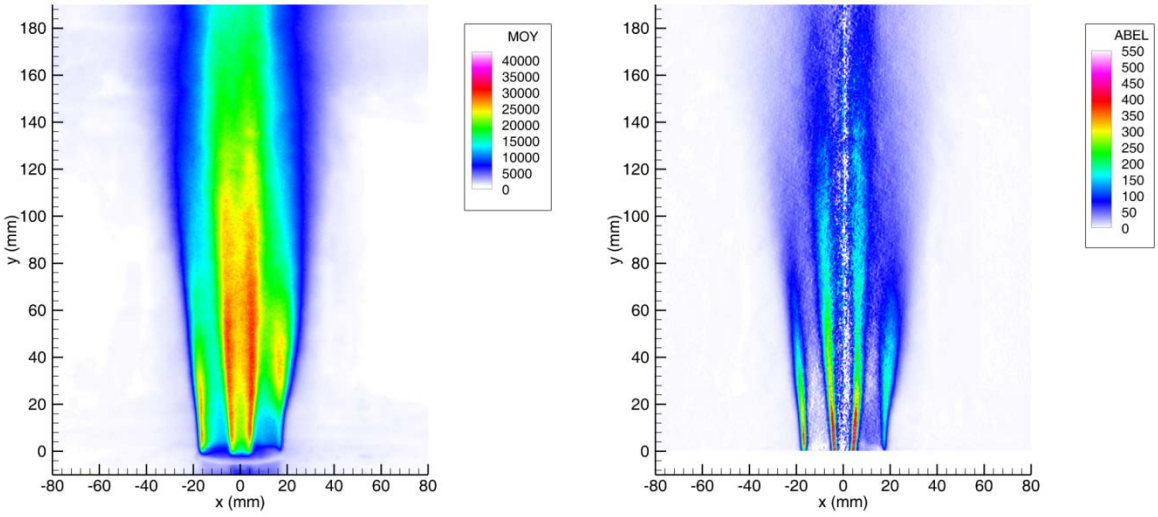

Figure 9. The structure of 'type B' oxyfuel BFG flame for 17.5kW, Ro of 40% and T_{pr} = 300K.
a: Mean OH* chemiluminescence image. b: Tomographic image from Abel's inversion.

a. b.

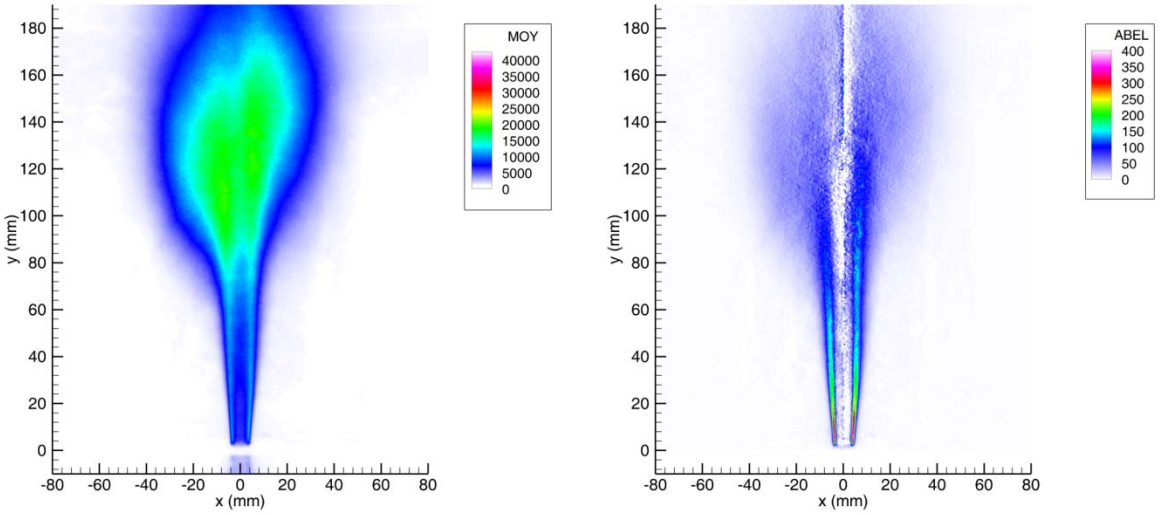

Figure 10. The structure of 'type C1' oxyfuel BFG flame for 23kW, Ro of 40% and T_{pr} = 300K.
a: Mean OH* chemiluminescence image. b: Tomographic image from Abel's inversion.

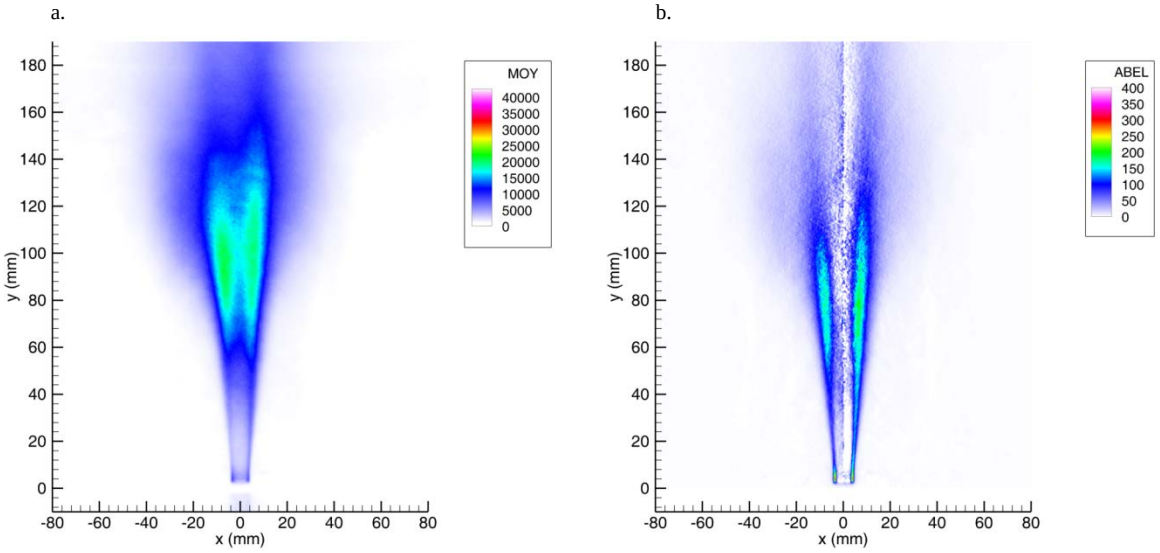

Figure 11. The structure of 'type C2' oxyfuel BFG flame for 23kW, Ro of 60% and T_{pr} = 300K
a: Mean OH* chemiluminescence image. b: Tomographic image from Abel's inversion.

The local intermittent stabilization and the flame extinctions result from the local features of mixing and shear in the BFG-O_2 layers, which are different for external and internal diffusion flames. The thin external oxygen annular flow with high velocity induces a rapid entrainment of combustion products recirculating in the furnace, which increases the dilution rate in the outer diffusion flame. This explains the appearance of local fluctuations (flame transition from A to B), followed by the external flame lifting-off (transition from B to C), whereas no effect of external dilution is expected at the central BFG-O_{2i} flame.

For this central BFG-O_{2i} flame, large Ro values may induce too large strain in the BFG-O_{2i} shear layer to stabilize a turbulent diffusion flame, when corresponding convection velocity U_{ci} is higher than U_c^*. This is brought out by drawing a second representation of the stability diagram with BFG and inner oxygen injection velocities (Figure

12). The transition between attached and lifted central BFG-O_{2i} flame corresponds then to the changeover from C1 flames (red filled triangles) to C2 flames (red open triangles). Considering that this transition occurs at a critical shear for the diffusion flame stabilization, the limit is expressed as the threshold value of the convection velocity $U_{Ci}{}^{*} = (U_{BFG}+U_{O2i})/2$ [Paubel 2007]. This value was experimentally determined from the stability diagram as 14.5 $m.s^{-1}$ at 300K, slightly higher than the previous one, 10.5 $m.s^{-1}$, which was obtained in a quadri-coaxial configuration with lower lip thickness (e = 0.5 mm), using a surrounding annular CH_4/O_2 flame [Paubel 2007].

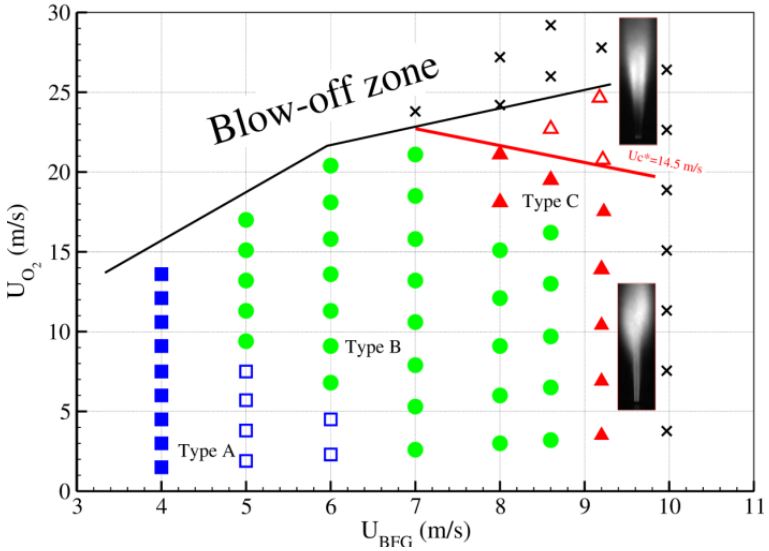

Figure 12. Stability diagram of oxyfuel BFG flames as function of BFG and inner oxygen injection velocities, U_{BFG} and U_{O2} respectively, without reactants preheating. (blue filled square: A1 flame - blue open square: A2 flame - green circle: B flame - red filled triangle: C1 flame - red open triangle: C2 flame - black cross: blown-off flame)

5.3. Stability diagram and flame structures with reactants preheating at 600K

The effect of reactant preheating on flame stabilization is illustrated in this section for both BFG and oxygen preheating temperature of 600 K. The same test procedure as for non-preheated experiments is carried out in order to produce the flame stability diagram presented in Figure 13. For this, having variations of the thermal power and increasing Ro, different flame structures and stability limits are obtained.

These results show clearly the benefits of reactants preheating. The presence of double attached A2 flames with low pollutant emissions is extended from 15 kW without reactants preheating, up to 25 kW such as it is shown in Figure 13. Same flame characteristics as fluctuating B flames, external lifted C flames or non-stable flames have also been observed, as in the non-reactants preheating case presented in Figure 7.

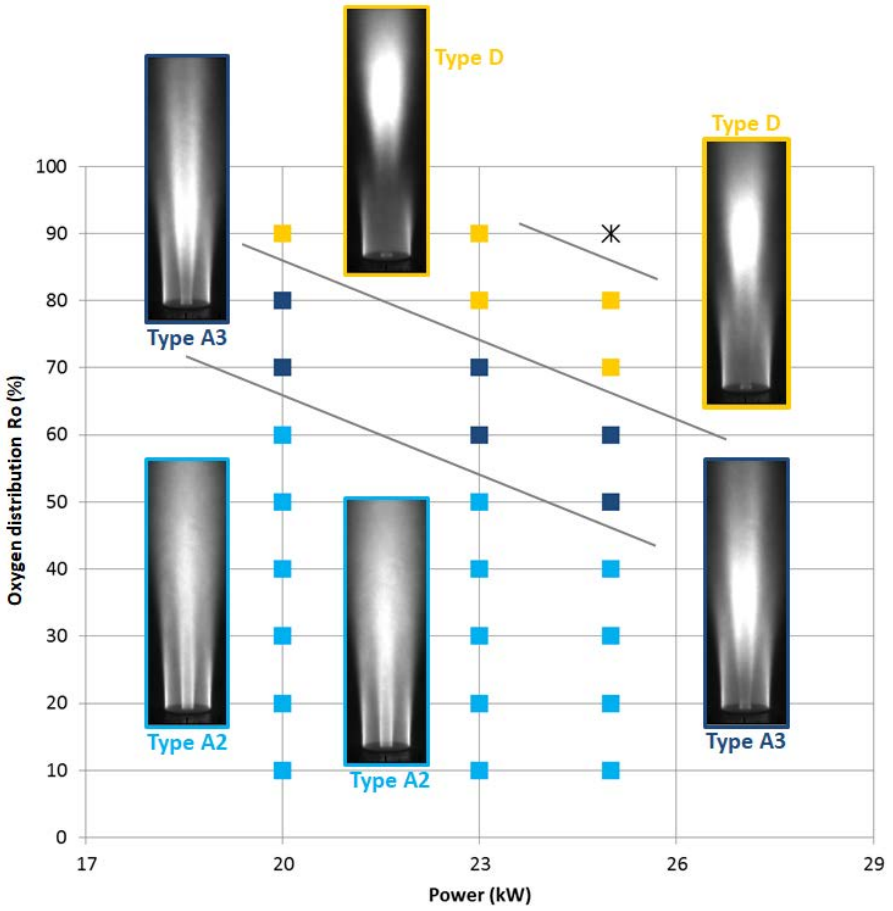

Figure 13. Stability diagram of oxyfuel BFG flames generated with reactant preheating at Tpr = 600 K. (light blue square: A2 flame - dark blue square: A3 flame - yellow square: D flame - black cross: blown-off flame)

Double attached flames A1 and A2 present similar topologies with maxima OH* chemiluminescence occurring directly from the burner exit (Figure 8). With reactants preheating, another sub-type A3 of double attached flame can be defined where the central BFG-O_{2i} flame exhibits a maximum of OH* chemiluminescence downstream from the burner exit shown in Figure 13. This occurs due to the large momentum flux in the central oxygen jet at high Ro value. At this condition an additional increase of thermal power, or of the inner oxygen injection raises the shear of the BFG-O_{2i} flame which is then lifted-off, whereas the outer BFG-O_{2e} flame is kept attached to the burner, leading to Type D structure observed in Figure 14. Therefore, the stability limit of preheated BFG oxyfuel flames seems to be more sensitive to the strain in the inner BFG-O_{2i} shear layer than to the strain in the outer BFG-O_{2e} shear layer. When increasing Ro, preheating of reactants makes the flame still stable even at higher momentum of the inner jet. This comes from the highly stable external BFG-O_{2e} flame, which acts as a protective pilot flame supplying sufficient heat to ensure the ignition of the internal BFG-O_{2i} flame downstream.

CO and NOx emissions measured in the flue gas reached very low levels, less than 15 ppm, for all reactants preheating temperatures. In addition to this, no significant changes are observed during the transitions between

flame types. This shows that the reactants preheating with oxyfuel combustion for flame stabilization has no negative impact on the environmental impact of LCV fuels combustion due to the presence of inert species in the fuel.

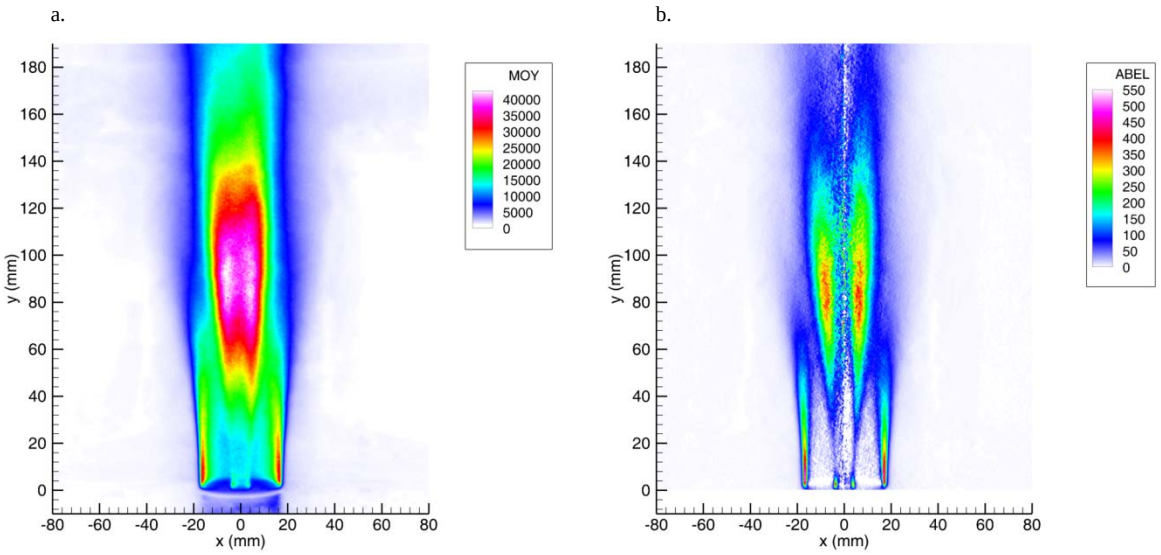

Figure 14. The structure of 'type D' oxyfuel BFG flame for 25kW, Ro of 60% and T_{pr} = 600K.
a: Mean OH* chemiluminescence image. b: Tomographic image from Abel's inversion.

5.4. Oxyfuel BFG flames stability limits with reactants preheating

The effect of the reactants preheating on the stability of an oxyfuel BFG diffusion flame is studied by analysing the transitions of the inner BFG-O_{2i} flame. For this, the stability diagrams and associated flames topology are presented on Figure 15 as a function of BFG and inner oxygen O_{2i} velocities for 3 thermal powers (respectively 20, 23 and 25 kW) at different preheating temperatures.

For these particular cases, there are no transitions between A type flames to B or C types, as shown previously when the reactants are preheated at 600K. For $T_{pr} \geq 400$ K, the limit of stability of the BFG-O_{2i} flame corresponds to the transitions between the A2 and the D flames. Then, the threshold value of the convection velocity $U_{Ci}^{*} = (U_{BFG}+U_{O2})/2$ is experimentally determined from each stability diagram as a linear limit between the A2 and the D flames (Figure 13). For each preheating temperature, the critical convection velocity U_{C}^{*} and the corresponding Damköhler number Da* are shown in the stability diagrams in Figure 15 where a significant increase of U_{C}^{*} with T_{pr} is observed. Whereas Damköhler number Da* is almost constant confirming the assumption adopted for the burner design methodology.

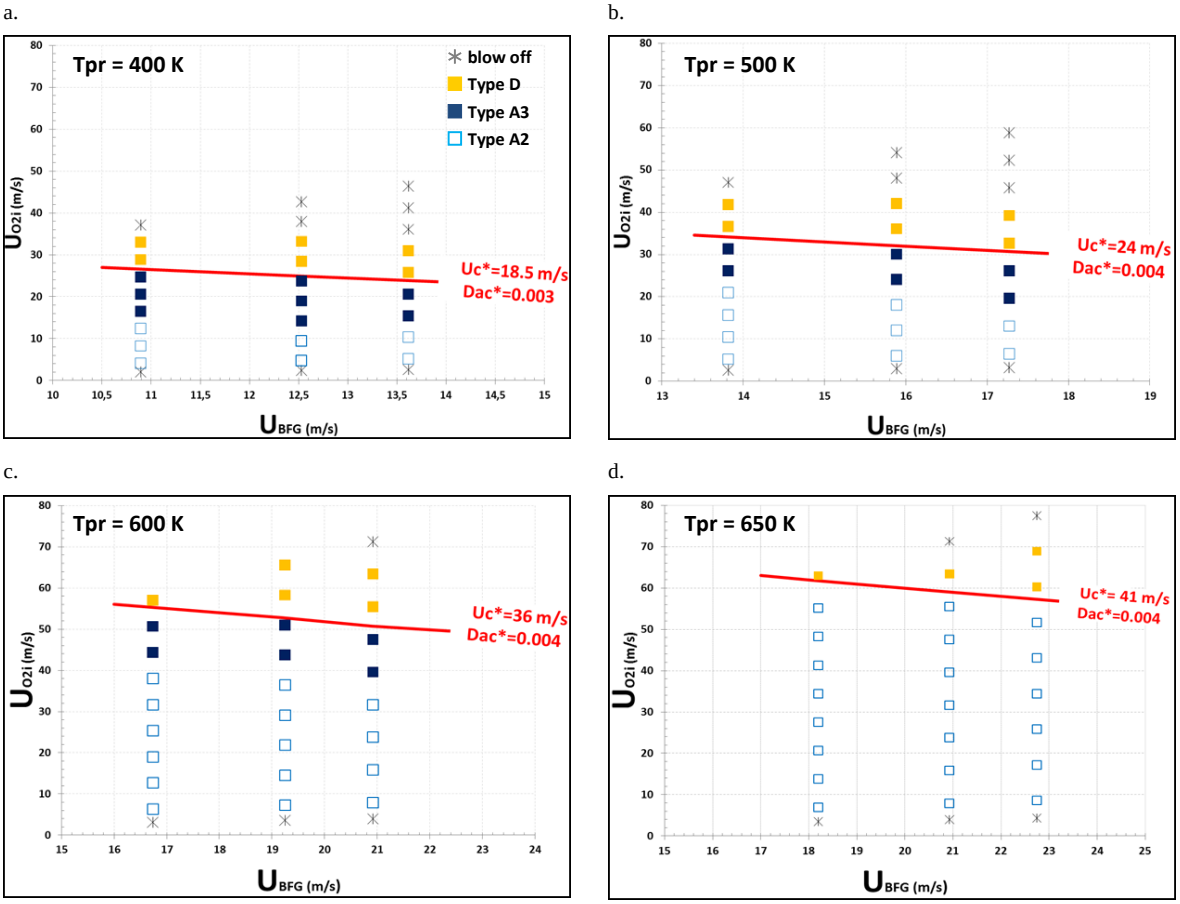

Figure 15. Stability diagrams of oxyfuel BFG flames as function of BFG and inner oxygen injection velocities, U_{BFG} and U_{O2i} respectively, with different preheating temperatures. (light blue square: A2 flame - dark blue square: A3 flame - yellow square: D flame - black cross: blown-off flame)

Variations of experimental critical convection velocities with reactants preheating temperature is gathered on Figure 16, and compared to the theoretical one obtained with the model presented in section 4.2. Considering the precision of the experimental analysis caused by the measurements uncertainties and the approximations of the theoretical model, a good agreement between the theoretical and experimental values at 25 kW is observed. These results show the substantial advantage provided by reactants preheating on the oxyfuel flame stability, as well as the model suitability to help on the design of a burner adapted to LCV fuels.

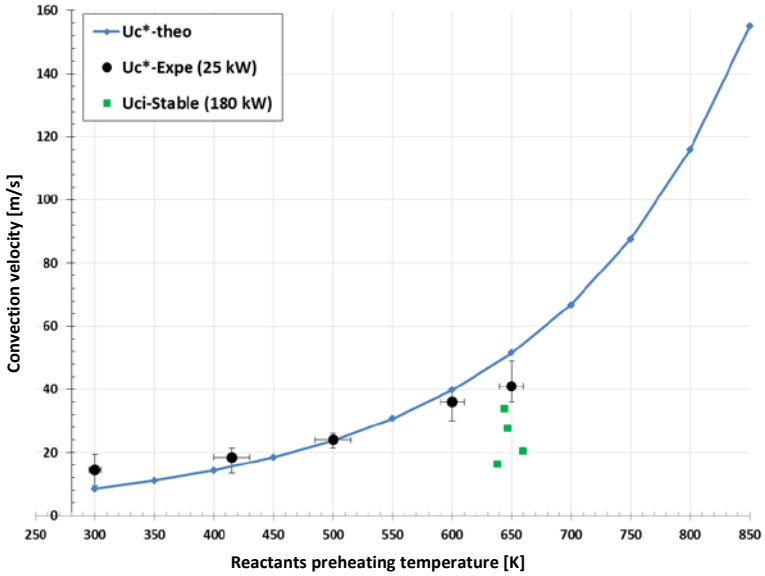

Figure 16. Convection velocity for the internal BFG-O_{2i} flame lifting vs. reactants preheating temperature for laboratory and semi industrial tests. . (black dots: critical values from lab-scale experiments – blue line: theoretical limit - green squares: convection velocity for stable semi-industrial experiments).

6. Scale-up from laboratory to semi-industrial facility

Complementary to the detailed experimental study of preheated BFG oxyfuel combustion performed at laboratory scale, a second experimental study is done at nominal industrial scale to assess the effect of scaling-up. The semi-industrial facility at Air Liquide R&D Centre consists of a horizontal cylindrical combustion chamber, 5 m long and internal diameter of 1.1 m. The facility is insulated with ceramic fiber (T_{max} = 1700K) and equipped with lateral port accesses for flame visualization and flue gases sampling. The large-scale burner has the same geometrical configuration as the lab-scale one, and its dimensions were determined from a scale-up methodology based on the criteria of critical convection velocity and flow velocity conservation for nominal operating conditions of 180 kW. Same BFG composition is chosen (Table 1) and is generated as a mixture from pure gases, such as the same procedure done at laboratory experiments. Two electric preheaters are used to enable continuous preheating of BFG and oxygen up to a maximum of 700 K and 823 K respectively.

The OH* chemiluminescence imaging is performed through the first lateral optical access, closed to the burner exit. The mean OH* image and its corresponding Abel's inverted image are presented on Figure 17 for the operating conditions corresponding to 180kW, Ro of 85%, T_{pr} (BFG) of 700K and $T_{pr}(O_2)$ of 550K. The same flame topologies as in the lab-scale experiments are observed. Preheating both reactants leads to the stabilization of a double attached flame, corresponding to a flame type A for all tested operating conditions, as they fulfilled the criteria of convection velocity lower than the critical one. These are shown as green squares, in Figure 16.

Tests within the burner turn-down ratio between 100 kW and 180 kW were done during the semi-industrial experiments, having in this range very stable and attached flames type A2; as well as NOx emissions around 60 ppm in all the cases.

Having in mind that 180 kW thermal power corresponds to the nominal capacity of burner for application in a reheating furnace of the steel making process; these results are first proof-of-concept of the advantage of the oxyfuel combustion combined with reactants preheating in order to reach flame stability of LCV fuels, at this industrial scale.

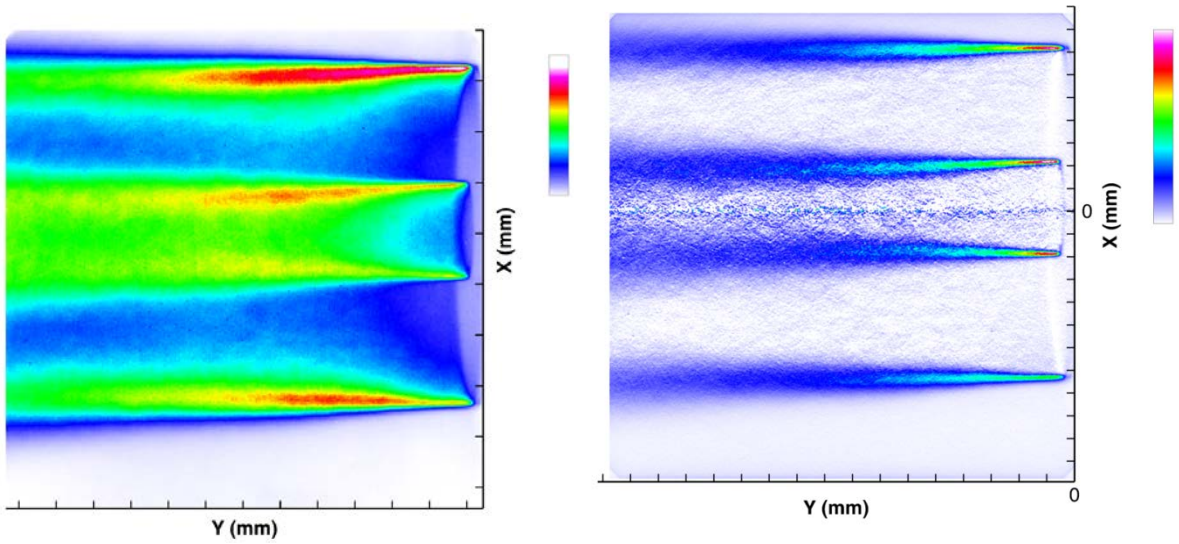

Figure 17. Oxyfuel BFG flame obtained on the semi-industrial facility under the conditions 180kW, Ro = 85%, Tpr(BFG) = 700K and Tpr(O_2) = 550K.
Left: Mean OH* chemiluminescence image. Right: Tomographic image reconstructed by Abel's inversion.

7. Conclusions

This paper presents an experimental study of turbulent flame stabilization of low calorific value fuel gas by oxyfuel combustion and reactants preheating. Characterisation of this alternative is based first on thermochemical calculations which show and quantify the potential benefit of the reactants preheating on the stabilization of oxyfuel LCV flames, throughout the increases in the adiabatic flame temperature, the laminar flame velocity and the impact on the strain rate which provides an extension of the operational range before the flame blow off. These results are used to develop an original methodology to design an oxyfuel LCV non-premixed burner, based on the theoretical criteria associated to a critical Damköhler number; and at the same time allows to qualify the enhancement of flame stability with reactant preheating.

Laboratory scale experiments demonstrate the advantage of oxyfuel combustion and reactants preheating for LCV flames stabilization. Different flame structures based on the oxygen distribution are identified from OH*

chemiluminescence imaging. Stable type A flames are obtained where the two flames in the BFG-O_2 shear layers are always attached to the burner exit. B and C flames occur when respectively the external flame presents some local intermittent extinction or is lifted-off. A type D flame is also observed where the internal flame lifts at a large critical convection velocity. A good agreement is obtained between the theoretical critical convection velocity and the experimental results. Very low CO and NOx emissions - less than 20 ppm - are measured in the flue gas for all relevant operating conditions. Complementary semi-industrial experiments show the same flame characteristics obtained at lab-scale, having always a double attached flame, corresponding to type A, for all operating conditions at nominal industrial scale. These results validate the characterization of the physical phenomena leading to flame stability and its quantification, as well as confirm the scale-up criteria used. In general, the combination of oxyfuel combustion with reactants preheating allows to optimise the use of alternative energy sources as the low calorific fuel gases on the steel manufacturing industrial plants, with potential energy savings, due to the reduction of natural gas consumption. Although this technology is originally proposed for the steelmaking industry, it can also be open to any other thermal process using low calorific value gases.

Acknowledgments

This study was performed in the framework of the 'CALOHRY' project joining Air Liquide, CMI GreenLine and CORIA laboratory, with the financial support of ANR (ANR-12-SEED-0010-01).

References

[1] T. Komori, N. Yamagami, H. Hara. International Gas Turbines Congress. Tokyo (2003).

[2] C. Li, H. Tang, L. Jing, M. Zhu. Journal of Engineering for Gas Turbines and Power. 138. DOI: 10.1115/1.4031348 (2015).

[3] A.P. Giles, R. Marsh, P.J. Bowen, A. Valera-Medina. Fuel 182: 531–540 (2016).

[4] O. Gicquel, L. Vervisch, G. Joncquet, B. Labegorre, N. Darabiha, Fuel 82: 983-991 (2003).

[5] S.S Hou, C.H. Chen, C.Y. Chang, C.W. Wu, J.J. Ou, T.H. Lin. Energy Conversion and Management 52: 2758–2767 (2011).

[6] X. Paubel, Analyse expérimentale des oxy-flammes turbulentes non-prémélangées de gaz bas PCI. PhD Thesis INSA de Rouen. 2007.

[7] X. Paubel, A. Cessou, D. Honore, L. Vervisch, R. Tsiava. Proc. Combust. Inst. 31: 3385-3392 (2007).

[8] Y. Joumani, B. Leroux, A. Contino, O. Douxchamps, J. Behen, Glass Int 33: 32-38 (2010).

[9] J-W. Moon, S-J. Kim and Y. Sasaki. ISIJ International, 54: 63-71 (2014).

[10] A. Bâ, A. Cessou, X. Paubel, D. Honoré. Proc. European Combustion Meeting, Budapest, Hungary, 2015.

[11] S.G. Davis, A.V. Joshi, H. Wang, F.N. Egolfopoulos. Proc. Combust Inst. 30: 1283-1292 (2005).

[12] Wang J., Huang Z. Kobayashi H., Ogami Y. International Journal of Hydrogen Energy 37 (2012).

[13] M. Juniper, S. Candel. Journal of Propulsion and Power 19: 332-341 (2003).

[14] Y. Otakeyama, T. Yokomori, M. Mizomoto. Proc. Combust Inst. 32:1091–1097 (2009).

[15] D.P. Mishra. Fuel 82 1471-1475 (2003).

[16] S.P. Sharma, D.D. Agrawal, C.P. Gupta. Proc. Combust Inst. 18: 493-501 (1981).

[17] P. Han, M. Checkel, B. Fleck, N. Nowicki. Fuel 86: 585–596 (2007).

[18] S. Liao, D. Jiang, Q. Cheng. Fuel 83: 1247–1250 (2004).

[19] F S. Lamige, K. M ; Lyons, C. Galizzi, M. Kühni, E. Mathieu, D. Escudié. Combust. Sci. And Technol. 187: 1937-58 (2015).

[20] S; Candel, M. Juniper, G. Singla, P. Scouflaire, C. Rolon. Combust. Sci. And Technol. 178:1-3, 161-192 (2007).

[21] W.J.A. Dahm, C.E. Frieler, G. Tryggvason. J. Fluid Mech. 241: 371–402 (1992).

[22] F. Takahashi, W.J. Schmoll. Proc. Combust. Inst. 23 (1990).

[23] H. Rehab, E. Villermaux, E.J. Hopfinger. J. Fluid Mech. 345: 357–381 (1997).

[24] E. Villermaux, H. Rehab, J. Fluid Mech. 425: 161–185 (2000).

[25] N. Peters. Turbulent Combustion. Cambridge University Press. 2000